

Nicotine as Corrosion Inhibitor for 1018 Steel in 1M HCl under Turbulent Conditions

Araceli Espinoza-Vázquez*, Sergio Garcia-Galan and Francisco Javier Rodríguez-Gómez

Faculty of Chemistry, Department of Metallurgical Engineering, Universidad Nacional Autónoma de México, C.U., Distrito Federal, 04510, Mexico

Abstract

An electrochemical impedance technique for determining corrosion inhibition of nicotine in HCl on AISI 1018 steel under concentrations from 0 to 50 ppm found that the organic compound is a better corrosion inhibitor under static conditions. The inhibition efficiency (IE) increased with inhibitor concentration reaching an IE>90%, at 10 ppm. For [nicotine] ≤ 50 ppm, the IE value reached 71%, at 40 rpm, but diminished then to 33% upon changing the working electrode rotation speed to 500 rpm. The thermodynamic analysis showed a process ruled by physisorption according to the Langmuir adsorption model mechanism. Furthermore, the inhibition kinetics study showed that nicotine gave good protection against corrosion up to 72 hours of immersion with IE ≤ 87%. Finally, with increased temperature the IE values diminished from 90% at 25°C to 57% at 70°C, concluding that at high temperatures nicotine is ineffective at inhibition, because the temperature decrease, persistence layer easily desorbs.

Keywords: AISI 1018 steel; Nicotine; Corrosion inhibition

Introduction

The transport of hydrocarbons in the oil industry depends on the use of pipelines that can be damaged by corrosion, causing large impacts on production, significant damage to property, as well as pollution, and risk to human lives [1].

Corrosion inhibitors [2-5], such as molybdates, phosphates, and ethanolamines, are effective, but they are very toxic. The development of corrosion inhibitors, non-toxic and compatible with the environment, is an area of great importance in the science and technology of corrosion [6-8]. Inhibitor substances extracted from plants offer environmental and cost advantages; for example alkaloid extracts from *Oxandra asbeckii* plant [9], *Hibiscus sabdariffa* [10], Geissospermum leave [11] *Euphorbia falcate* [12] show 89% inhibition efficiency, *Morinda tinctoria* has a 70% at 30% v/v [13]; they have been tested, but there is a lack in assessing and identifying the active substance.

Nicotine ((S)-3-(1-methylpyrrolidin-2-yl) pyridine) is an organic compound belonging to the alkaloids: a liquid, oily, and colorless derivative of the ornitina, Figure 1, synthesized in the areas of high activity in the roots of tobacco plants, and transported by the sap to the greens. Structurally, this compound is formed by a pyridine and a pyrrole that could have bifunctional activity from nitrogen atoms. Given its chemical structure, this organic compound is a candidate for the protection of petroleum pipeline systems, since it is of natural origin, readily found in tobacco plants (*nicotiana tabacum*), in which it is the major active chemical component. Furthermore, the *nicotiana tabacum* extract has been reported by Njokua et al. and they demonstrated that the best concentration was 1200 mg/L with 89% IE [14] and Bhawar et al. [15] found to have inhibitory corrosion properties for mild steel in acidic medium, attaining 94.13% IE at an optimum concentration of 10 g/L under static conditions for 6 hours at 303 K.

In the oil industry the hydrocarbon flow is typically turbulent, when the Reynolds number (Re) is greater than 1000. Laboratory standard testing (ASTM G170 and ASTM G-185) of corrosion inhibitors using rotating cylinder electrodes recommend flow rates from 100 to 500 rpm corresponding to hydrocarbon transport of 194 and 970 L/min, respectively.

Many substances, able to be adsorbed, have been introduced

as corrosion inhibitors, for example azol derivatives [16-20], so it is important to evaluate candidates to determine the conditions under which they might be effective.

Consequently, our interest in evaluating this organic molecule as pure compound has been demonstrated inhibition properties against corrosion thus making it an eco-friendly material equally proper for engineering uses under different hydrodynamic conditions and temperatures, which simulates the transport of hydrocarbons.

The inhibition efficiency of nicotine, IE, can be calculated as [21]:

$$IE / \% = \frac{\left(\frac{1}{R_p}\right)_{\text{blank}} - \left(\frac{1}{R_p}\right)_{\text{inhibitor}}}{\left(\frac{1}{R_p}\right)_{\text{blank}}} \times 100 \quad (1)$$

where R_p is the polarization resistance with ("inhibitor") or without inhibitor ("blank").

The value of polarization resistance is an important parameter that can be obtained from electrochemical impedance spectroscopy to estimate the rate of corrosion, by using small polarization, i.e., no damage on the electrode is caused due to experiment.

Materials and Methods

Inhibitor solution 0.01M nicotine (Aldrich 97% purity) was prepared in water, with different aliquots taken from this solution, with concentrations ranging from 5 to 50 ppm added to the 1M HCl

*Corresponding author: Araceli Espinoza-Vázquez, Faculty of Chemistry, Department of Metallurgical Engineering, Universidad Nacional Autónoma de México, C.U., Distrito Federal, 04510, Mexico, Tel: 52-55-56225225; E-mail: arasv_21@yahoo.com.mx

Received August 26, 2015; Accepted September 30, 2015; Published October 07, 2015

Citation: Espinoza-Vázquez A, Garcia-Galan S, Rodríguez-Gómez FJ (2015) Nicotine as Corrosion Inhibitor for 1018 Steel in 1M HCl under Turbulent Conditions. J Anal Bioanal Tech 6: 273. doi:10.4172/2155-9872.1000273

Copyright: © 2015 Espinoza-Vázquez A, et al. This is an open-access article distributed under the terms of the Creative Commons Attribution License, which permits unrestricted use, distribution, and reproduction in any medium, provided the original author and source are credited.

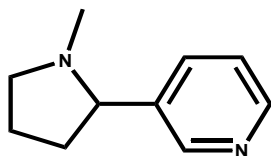


Figure 1: Chemical structure of nicotine.

electrolyte, prepared through dilution of the HCl analytical grade reagent at 37% with doubly distilled water.

The electrochemical impedance study was performed at room temperature using the Gill AC workstation, applying a sinusoidal ± 10 mV perturbation, within the 10^{-1} Hz to 10^4 Hz frequency range to an electrochemical cell with a three-electrode setup. A saturated Ag / AgCl electrode was used as reference, with a graphite rod as counter electrode, while the working electrode (rotating cylinder electrode, RCE) was the AISI 1018 steel sample with ~ 3.92 cm² exposed area, duly prepared through standard metallographic procedures. The working electrode was first immersed into the test solution for 30 min to establish steady-state open-circuit potential.

The study under hydrodynamic conditions was carried out at 0, 40, 100 and 500 rpm. In addition, a study of kinetic inhibition of nicotine (50 ppm) for immersion times of 30 days maximum was performed, observing the effect of temperature at the same concentration from 30 to 70°C, with $\pm 2^\circ\text{C}$ error.

Results and Discussion

Effect of concentration

Figure 2a shows impedance diagrams for the immersed metal, with an increase in the value of Z_{re} at higher rotation rates in 1M HCl due to the increase of mass transfer and localized attack [22].

Figure 2b-2e show the results for different rotation rates; the diameters of semicircles in Nyquist plots increase with increasing the inhibitor concentration. Analysis of the shape of the Nyquist plots revealed the curves were approximated by two semicircles: one time-constant at high frequency associated with a corrosion process, while the second time-constant at low frequency would likely be associated with inhibitor adsorption [23,24].

When the RCE was at static condition (0 rpm) and at 10 ppm a Z_{re} of 900 $\Omega\cdot\text{cm}^2$ was found, slightly increasing to 1000 $\Omega\cdot\text{cm}^2$ at 50 ppm. On the other hand, at 100 rpm, Figure 2d, Z_{re} decreases to 350 $\Omega\cdot\text{cm}^2$ at 50 ppm, attributable to a desorption of organic molecules on the electrode surface [25].

To determine electrochemical parameters of nicotine for different rotation rates (static and turbulent flows), simulation using electrical circuits was carried out using the Zview program, which are shown in Figure 3. Electrical equivalent-circuit diagram in Figure 3a corresponds to the metal/solution interface (double layer between the metallic surface and acid solution). Figure 3b describes a two-time-constant model, corresponding to the metal/solution interface and the inhibitor adsorption. R_s is the solution resistance, R_{ct} the charge transfer resistance, R_{mol} the molecular resistance, CPE_1 and CPE_2 the constant phase elements corresponding to the R_{mol} and R_{ct} , respectively.

The value of polarization resistance is calculated as:

$$Z_{CPE} = Y_0^{-1} (j\omega)^{-n} \quad (2)$$

For the description of a frequency-independent phase shift between an applied AC potential and its current response, a constant phase element (CPE) is used, which is defined in impedance representation as:

$$Z_{CPE} = Y_0^{-1} (j\omega)^{-n} \quad (3)$$

where Y_0 is the CPE_1 or CPE_2 , n is the CPE exponent that can be used as a gauge of the heterogeneity or roughness of the surface, j the unit imaginary number, and ω is the angular frequency in rad/s. Depending on n , CPE can represent a resistance ($Z_{CPE}=R$, $n=0$); capacitance ($Z_{CPE}=C$, $n=1$); a Warburg impedance ($Z_{CPE}=W$, $n=0.5$); or inductance ($Z_{CPE}=L$, $n=-1$). The equation to convert Y_0 into double layer capacitance (C_{dl}) is given by ref. [26-28]:

$$C_{dl} = Y_0 (\omega_{max})^{n-1} \quad (4)$$

Tables 1-4 show the corresponding values from the simulation of the experimental data, demonstrating that in all cases the concentration has greater polarization resistance compared with non-inhibitor.

Adequate corrosion protection was found when nicotine was assessed under static conditions, since at 10 ppm it reached 90%, attributable to the organic compound being adsorbed more easily under these conditions.

However, for rotation rates greater than 40 rpm (turbulent flow) the polarization resistance and the inhibition efficiency were reduced. This effect could be due to the high Reynolds number regime causing the partial desorption of inhibitor at higher wall shear stresses [29,30].

Thus, Table 1 indicates that C_{dl} decreases at greater inhibitor concentration, because increase the thickness of the inhibitor layer or decrease in local dielectric constant [31,32]. Also, inhibition efficiency is higher than for turbulent flow (Tables 2-4). Therefore, with agitation the inhibitor-adsorbed layer is thinner than in static conditions, and even be heterogeneous and non-persistent. It can be assumed that the decrease of C_{dl} is caused by the gradual replacement of water molecules by adsorption of inhibitor molecules on the mild steel surface [33,34].

Figure 4 shows the IE at different rotation rates, noting that good protection is achieved in the static condition, reaching 90% IE at 10 ppm, attributed to the presence of electrodonor groups (pairs of free electrons in atoms in nitrogen) that favor the adsorption of nicotine on the metal surface.

Adsorption process

The adsorption of organic compounds can be described by two types of interaction: physisorption and chemisorption [35]. To determine the value of the standard Gibbs energy (ΔG_{ads}°) we used Equations 5 and 6, where K_{ads} is the adsorption equilibrium constant and θ is surface coverage, R is the universal gas constant, C is inhibitor molar concentration and T is the absolute temperature:

$$\frac{C}{\theta} = \frac{1}{K_{ads}} + C \quad (5)$$

$$\Delta G_{ads}^\circ = -RT \ln K_{ads} \quad (6)$$

The results in Table 5 indicate that the process is physisorption (electrostatic interaction), since the value of ΔG_{ads}° obtained from the linear fit shown in Figure 5 is less than -20 kJ/mol for the four-rotation rates tested [36-39].

Strong correlation coefficient ($R^2 \geq 0.9979$) of the Langmuir adsorption isotherm for nicotine was observed. The Langmuir

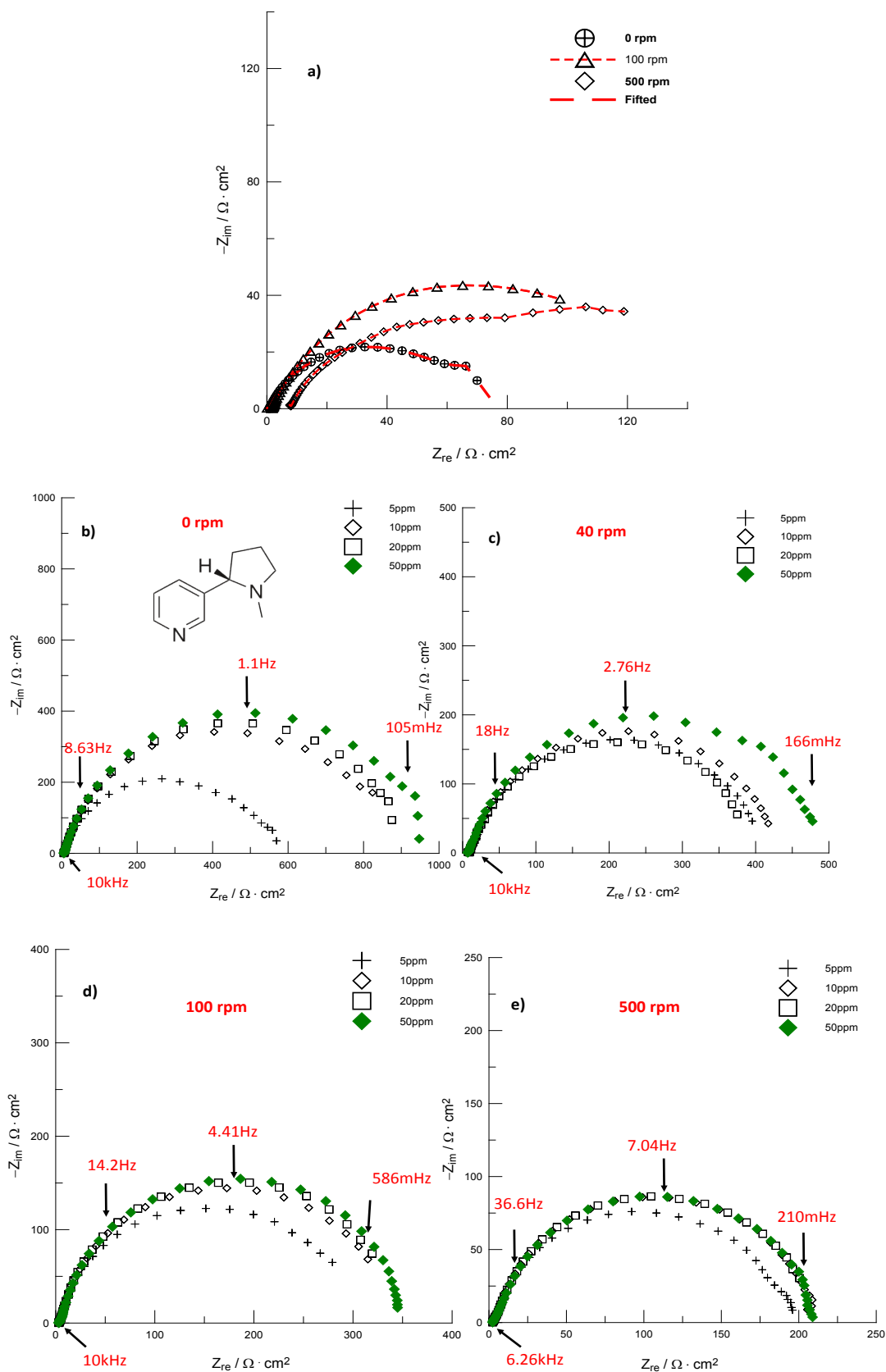
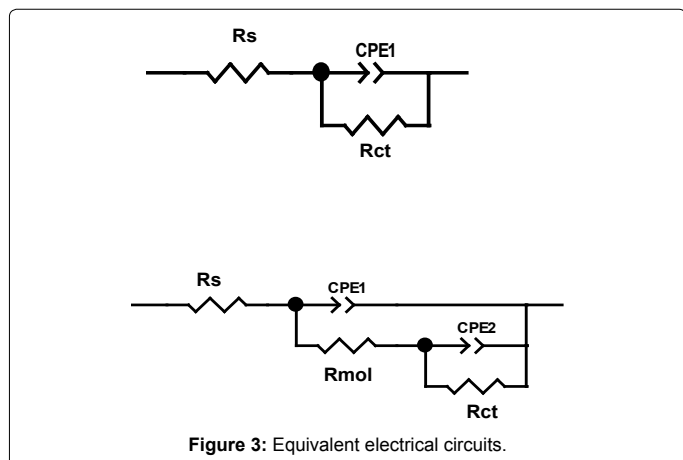


Figure 2: Nyquist diagrams at different concentrations of nicotine as a corrosion inhibitor at different rotation rates.



C/ppm	Rs/ Ω cm ²	n	Cdl/ μ F cm ²	Rp/ Ω cm ²	IE/%
0	3.4	0.8	351.0	83.0	-
5	6.4	0.9	81.6	552.7	85.0
10	6.2	0.9	71.4	878.1	90.5
20	6.2	0.9	69.2	907.1	90.8
50	6.1	0.9	72.4	974.1	91.5

Table 1: Electrochemical parameters of nicotine (0 rpm).

C/ppm	Rs/ Ω cm ²	n	Cdl/ μ F cm ²	Rp/ Ω cm ²	IE/%
0	8.5	1.0	400.3	141.1	0.0
5	10.9	0.9	392.2	403.8	65.0
10	9.5	0.9	432.5	431.2	67.3
20	8.9	0.8	441.0	394.7	64.3
50	7.6	0.8	429.9	490.8	71.2

Table 2: Electrochemical parameters of nicotine/solution interface (40 rpm).

C/ppm	Rs/ Ω cm ²	n	Cdl/ μ F cm ²	Rp/ Ω cm ²	IE/%
0	3.3	0.8	435.3	117.6	0.0
5	3.4	0.9	374.1	308.4	61.9
10	3.4	0.9	396.8	337.1	65.1
20	3.5	0.9	431.5	349.2	66.3
50	3.5	0.9	489.2	355.9	67.0

Table 3: Electrochemical parameters of nicotine/solution interface (100 rpm).

C/ppm	Rs/ Ω cm ²	n	Cdl/ μ F cm ²	Rp/ Ω cm ²	IE/%
0	8.5	1.0	760.0	141.1	0.0
5	2.9	0.9	314.9	191.1	26.1
10	2.8	0.9	372.9	206.9	31.8
20	2.6	0.9	462.9	210.5	33.0
50	2.6	0.9	515.8	210.7	33.0

Table 4: Electrochemical parameters of nicotine/solution interface (500 rpm).

adsorption isotherm assumes that the adsorption of organic molecules on the adsorbent is a monolayer. The high values of the adsorption equilibrium constant reflect the high adsorption ability of the nicotine molecules on the steel surface.

Effect of immersion time

Corrosion inhibitors are often evaluated in order to determine their performance under different conditions, such as the concentration, but few evaluated for persistence of the layer inhibitor. It is important to study the effect of immersion time to optimize concentration [40,41].

In the Nyquist plot of Figure 6, some examples of impedance curves at three different immersion times in the presence of 50 ppm of nicotine in 1M HCl are shown, with 24 hours of immersion producing a maximum Z_{re} value of 854 Ω -cm². After that time, this value decreases; at 240 hours it is remarkable to observe two time-constants, one attributed to the charge transfer resistance (corrosion process) and a second time-constant corresponding to an adsorbed molecular layer [42]. In Table 6, the values of corresponding resistances for each immersion time are summarized.

In order to clarify the behavior of nicotine (50 ppm) as a function of immersion time, Figure 7, a maximum inhibition period of 72 hours

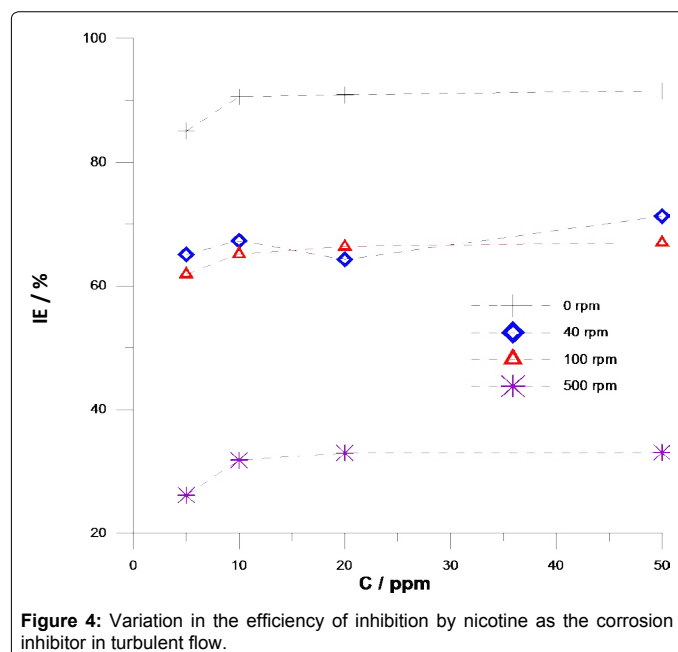


Figure 4: Variation in the efficiency of inhibition by nicotine as the corrosion inhibitor in turbulent flow.

Rotation rate/rpm	Ln k_{ads}	$\Delta G^{\circ}_{ads}/KJ mol^{-1}$	Regression Equation Lineal/mM	R ² (correlation coefficient)
0	5.77	-13.11	C/ θ =1.0864 C+0.0031	0.9999
40	4.16	-9.44	C/ θ =1.3839 C+0.0156	0.9979
100	5.13	-11.65	C/ θ =1.4812 C+0.0059	1
500	3.61	-8.21	C/ θ =2.9628 C+0.0269	0.9795

Table 5: Thermodynamic analysis of nicotine at different rotation rate by the Langmuir adsorption model.

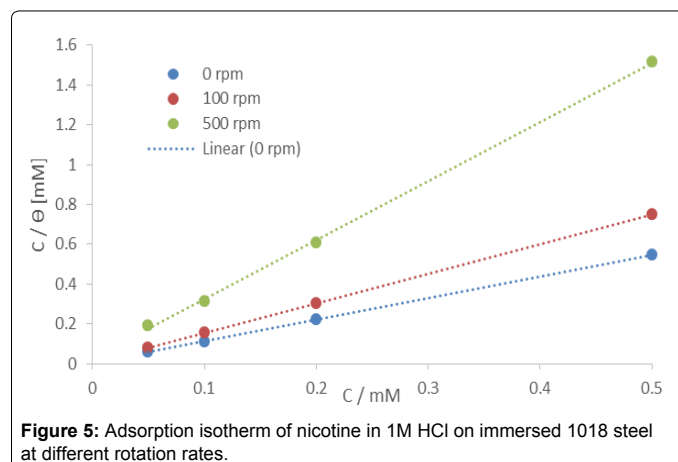


Figure 5: Adsorption isotherm of nicotine in 1M HCl on immersed 1018 steel at different rotation rates.

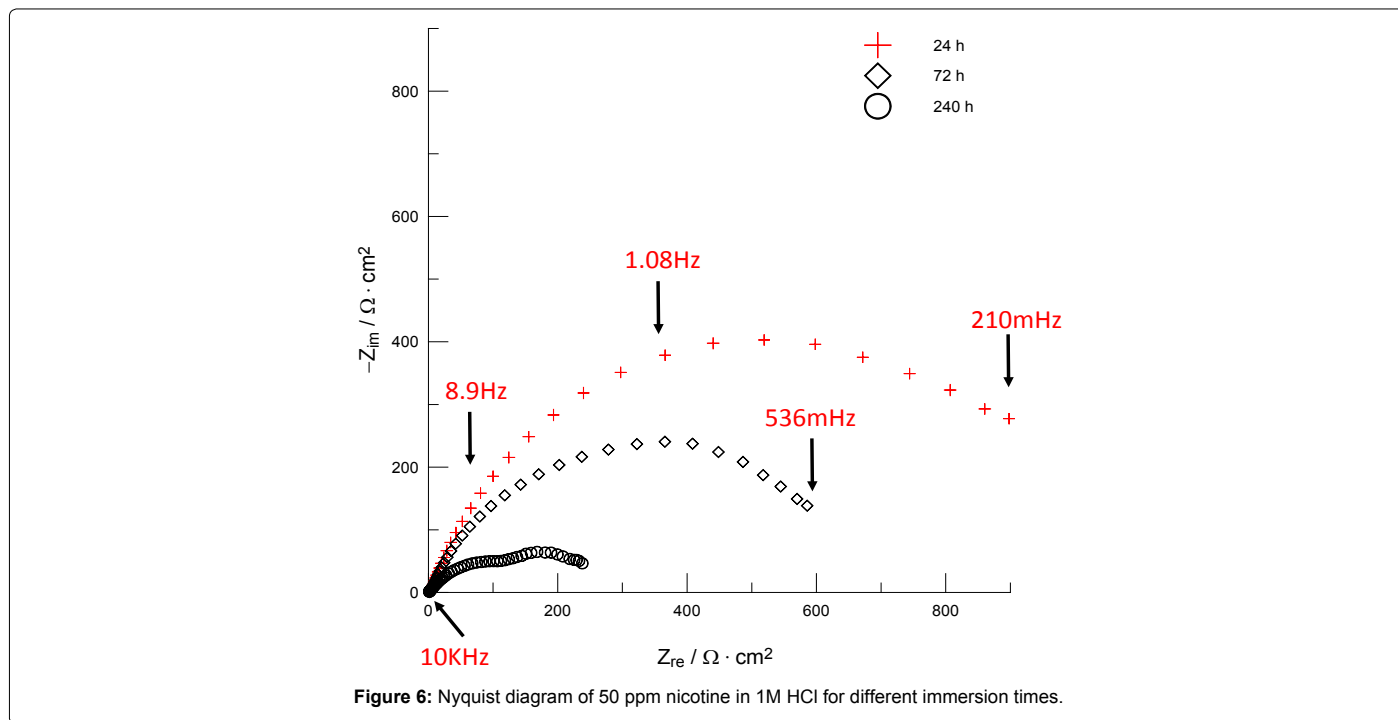


Figure 6: Nyquist diagram of 50 ppm nicotine in 1M HCl for different immersion times.

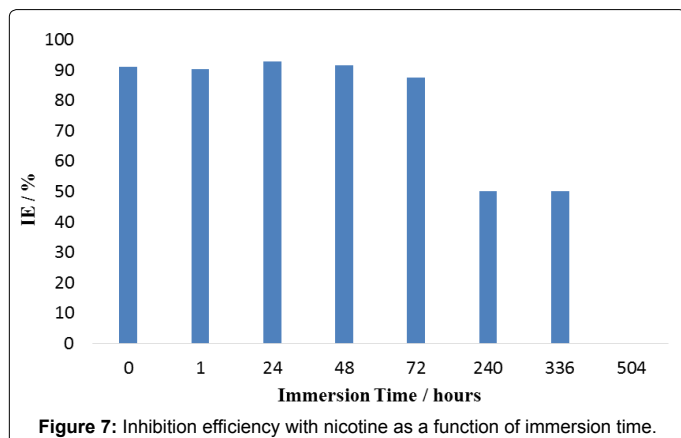


Figure 7: Inhibition efficiency with nicotine as a function of immersion time.

t/h	$R_{ct}/\Omega \cdot \text{cm}^2$	$R_{mor}/\Omega \cdot \text{cm}^2$	IE/%
1	854.0	5.9	90.3
24	1145.0	1.9	92.8
48	999.2	6.5	91.7
72	661.7	4.4	87.5
240	166.5	106.4	50.2
336	166.5	106.3	50.2
504	77.5	52.6	-

Table 6: Performance parameters of nicotine as a function of immersion time at 50 ppm.

T/C	$R_{ct, blank}/\Omega \cdot \text{cm}^2$	$R_{ct, inh.}/\Omega \cdot \text{cm}^2$	IE/%
30	188.0	510.0	63.1
40	141.2	525.3	73.1
50	71.91	371.7	80.7
60	23.7	105.0	77.4
70	45.0	105.1	57.2

Table 7: Effect of temperature in the presence of 50 ppm of 1M nicotine in HCl.

provides adequate protection (87%), after which this value decreases considerably to ~50%, due to a degradation of the nicotine adsorbed during the corrosion process.

Effect of Temperature

It has been observed that temperature can modify the interaction between the metal and the inhibitor [43]. In Figure 8, Nyquist plots are shown corresponding to: a) steel immersed in 1M HCl, and b) steel immersed in 50 ppm nicotine in the corrosive medium, at different temperatures.

Figure 8a shows that the value of Z_{re} decreases with increasing temperature, attributable to the 1M HCl solution causing material (steel) loss due to a faster corrosion process. When the inhibitor is added (50 ppm at Figure 8b), the previously mentioned effect in immersion time with temperature is also shown, with low charge transfer resistance at high temperature, as can be seen in Table 7. This fact is attributed to the inhibitor formed on the metal surface, thus a decrease in strength of the adsorption process at elevated temperature, suggesting physical adsorption [44] or desorption of the organic molecules (nicotine) at higher temperatures [45].

Conclusion

It was demonstrated that nicotine is an efficient corrosion inhibitor in HCl under static conditions, but only up to 10 ppm with efficiencies around ~ 90%. However, turbulent flow conditions (>40 rpm) affected the corrosion inhibition with IE less than 70%.

The nicotine is adsorbed on the metallic surface consistent with the Langmuir isotherm model.

The inhibitors behavior is affected with increase in temperature decreasing the persistence of the layer due to desorption process; according to the ASTM G 170 standard, this inhibitor is not suitable for high temperatures.

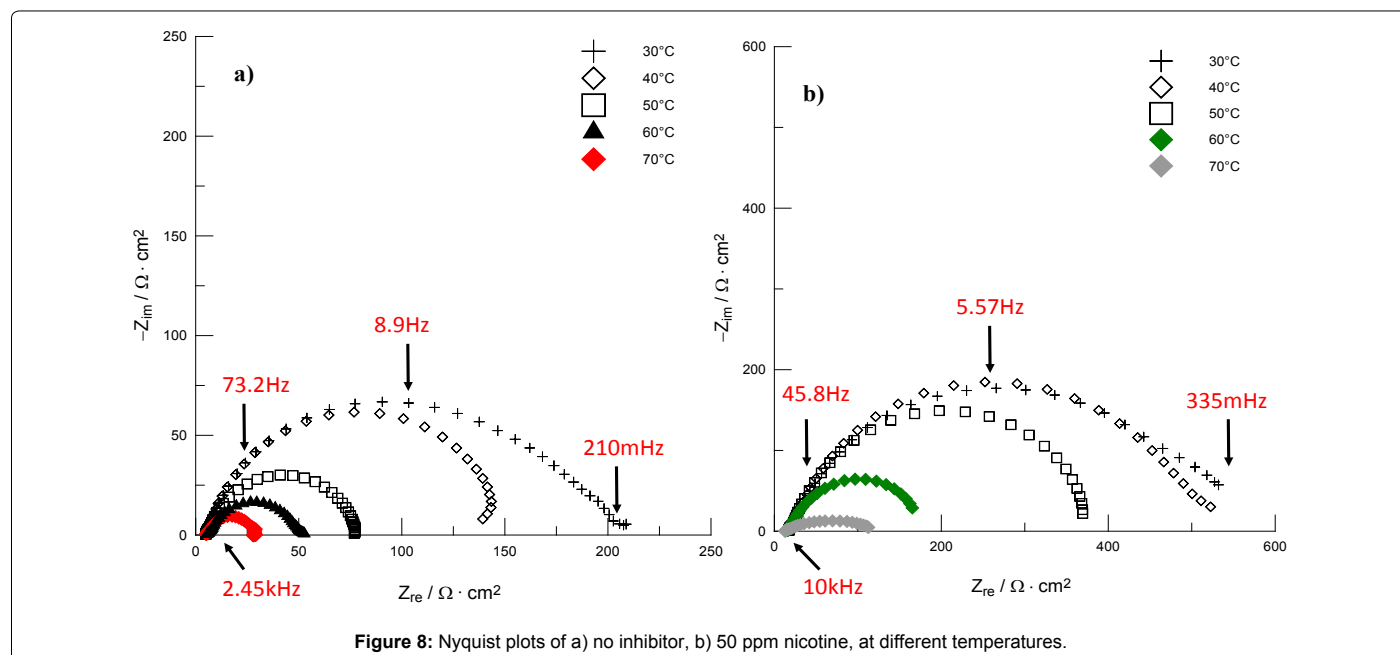


Figure 8: Nyquist plots of a) no inhibitor, b) 50 ppm nicotine, at different temperatures.

According to the ASTM G48 or G78 standard, the inhibitor is accepted when there is persistence of a test layer after 72 hours immersion. The inhibitors for this research meet that criterion.

Acknowledgements

The authors are grateful to the Faculty of Chemistry (UNAM), Department of Metallurgy and DGAPA for a postdoctoral fellowship for the corresponding author. AEV and FJRG wish to acknowledge the SNI (Sistema Nacional de Investigadores) for the honor of membership and the stipends received.

References

- Espinoza A, Negrón GE, González R, Angeles D, Herrera H, et al. (2014) Mild steel corrosion inhibition in HCl by di-alkyl and di-1H-1,2,3-triazole derivatives of uracil and thymine. *Mat Chem Phys* 145: 407-417.
- Yurt A, Bereket G, Kivrak A, Balaban A, Erk B (2005) Effect of Schiff bases containing pyridyl group as corrosion inhibitors for low carbon steel in 0.1 M HCl. *J App Electrochem* 35: 1025-1032.
- Awad MI (2006) Eco-friendly corrosion inhibitors: Inhibitive action of quinine for corrosion of low carbon steel in 1M HCl. *J of Appl Electrochem* 36: 1163-1168.
- Thiraviyam P, Kannan K (2013) Inhibition of Aminocyclohexane Derivative on Mild Steel Corrosion in 1N HCl. *Arab J Sci Eng* 38: 1757-1767.
- Tansug G, Tüken T, Sigircik G, Findikkiran G, Giray ES, et al. (2015) Methyl 3-((2-mercaptophenyl) imino) butanoate as an effective inhibitor against steel corrosion in HCl solution. *Ionics* 21: 1461-1475.
- Khadraoui A, Khelifa A, Hamitouche H, Mehdaoui R (2014) Inhibitive effect by extract of *Mentha rotundifolia* leaves on the corrosion of steel in 1M HCl solution. *Res Chem Intermed* 40: 961-972.
- El Ouariachi E, Bouyanzer A, Salghi R, Hammouti B, Desjobert J-M, et al. (2015) Inhibition of corrosion of mild steel in 1 M HCl by the essential oil or solvent extracts of *Ptychotis verticillata*. *Res Chem Intermed* 41: 935-946.
- Raja PB, Kaleem A, Abdul A, Awang K, Ropi M, et al. (2013) Indole Alkaloids of *Alstonia angustifolia* var. *latifolia* as Green Inhibitor for Mild Steel Corrosion in 1M HCl Media. *JMEPEG* 22: 1072-1078.
- Lebrini M, Robert F, Lecante A, Roos C (2011) Corrosion inhibition of C38 steel in 1 M hydrochloric acid medium by alkaloids extract from *Oxandra asbeckii* plant. *Corros Sci* 53: 687-695.
- Oguzie E (2008) Corrosion inhibitive effect and adsorption behaviour of *Hibiscus sabdariffa* extract on mild steel in acidic media. *Portug Electro Acta* 26: 303-314.
- Faustin M, Maciuk A, Salvin P, Roos C, Lebrini M (2015) Corrosion inhibition of C38 steel by alkaloids extract of *Geissospermum laeve* in 1M hydrochloric acid: Electrochemical and phytochemical studies. *Corros Sci* 92: 287-300.
- El Bribri A, Tabyaoui M, Tabyaoui B, El Attari H, Bentiss F (2013) The use of *Euphorbia falcata* extract as eco-friendly corrosion inhibitor of carbon steel in hydrochloric acid solution. *Mat Chem Phys* 141: 240-247.
- Krishnaveni K, Ravichandran J (2014) Influence of aqueous extract of leaves of *Morinda tinctoria* on copper corrosion in HCl medium. *J Electroanal Chem* 735: 24-31.
- Bhawsar J, Jain PK, Jain P (2015) Experimental and computational studies of *Nicotiana tabacum* leaves extract as green corrosion inhibitor for mild steel in acidic medium. *Alex Eng J* 54: 769-775.
- Njokua DI, Chidiebere MA, Oguzie KL, Ogukwe CE, Oguzie EE (2013) Corrosion inhibition of mild steel in hydrochloric acid solution by the leaf extract of *Nicotiana tabacum*. *Adv Mater Corros* 1: 54-61.
- Palomar MP, Romo MR, Hernández HH, Abreu-Quijano MA, Likhanova NV, et al. (2012) Influence of the alkyl chain length of 2 amino alkyl 1,3,4, thiadiazole compounds on the corrosion inhibition of Steel immersed in sulfuric acid solutions. *Corros Sci* 54: 231-243.
- Popova A, Christov M, Zvetanova A (2007) Effect of the molecular structure on the inhibitor properties of azoles on mild steel corrosion in 1M hydrochloric acid. *Corros Sci* 49: 2131-2143.
- Elayyachy M, Elkodadi M, Aouniti A, Ramdani A, Hammouti B, et al. (2015) New bipyrazole derivatives as corrosion inhibitors for steel in hydrochloric acid solutions. *Mat Chem Phys* 93: 281-285.
- Danaee I, Gholami M, RashvandAvei M, Maddahy MH (2015) Quantum chemical and experimental investigations on inhibitory behavior of amino-imino tautomeric equilibrium of 2-aminobenzothiazole on steel corrosion in H₂SO₄ solution. *J Ind Eng Chem* 26: 81-94.
- Bouklah M, Attayibat A, Kertit S, Ramdani A, Hammouti B (2005) A pyrazine derivative as corrosion inhibitor for steel in sulphuric acid solution. *App Surf Sci* 242: 399-406.
- Ameh PO, Eddy NO (2014) *Commiphora pedunculata* gum as a green inhibitor for the corrosion of aluminium alloy in 0.1 M HCl. *Res Chem Intermed* 40: 2641-2649.
- Khan PF, Shanthy V, Babu RK, Muralidharan S, Barik RC (2015) Effect of benzotriazole on corrosion inhibition of copper under flow conditions. *J Environ Chem Eng* 3: 10-19.
- Khaled KF (2008) Guanidine derivative as a new corrosion inhibitor for copper in 3% NaCl solution. *Mat Chem Phys* 112: 104-111.

24. Mahdavian M, Ashhari S (2010) Corrosion inhibition performance of 2-ercaptobenzimidazole and 2-mercaptobenzoxazole compounds for protection of mild steel in hydrochloric acid solution. *Electrochimica Acta* 55: 1720-1724.
25. Wang X (2012) The Inhibition Effect of Bis-Benzimidazole Compound For Mild Steel in 0.5M HCl Solution. *Int J Electro Sci* 71: 11149-11160.
26. Ouici H, Benali O, Harek Y, Larabi L, Hammouti B, et al. (2013) The effect of some triazole derivatives as inhibitors for the corrosion of mild steel in 5% hydrochloric acid. *Res Chem Intermed* 39: 3089-3103.
27. Lopez DA, Simison SN, de Sánchez SR (2003) The influence of steel microstructure on CO₂ corrosion. EIS studies on the inhibition efficiency of benzimidazole. *Electrochimica Acta* 48: 845-854.
28. Hassan HH (2007) Inhibition of mild steel corrosion in hydrochloric acid solution by triazole derivatives: Part II: Time and temperature effects and thermodynamic treatments. *Electrochimica Acta* 53: 1722-1730.
29. Barmatov E, Hughes T, Nagl M (2015) Efficiency of film-forming corrosion inhibitors in strong hydrochloric acid under laminar and turbulent flow conditions. *Corros Sci* 92: 85-94.
30. Gopiraman M, Sakunthala P, Kesavan D, Alexramani V, Kim IS, et al. (2012) An investigation of mild carbon steel corrosion inhibition in hydrochloric acid medium by environment friendly green inhibitors. *J Coat Technol Res* 9: 15-26.
31. Joseph A, Mohan R (2014) Electroanalytical and computational studies on the corrosion inhibition behavior of ethyl (2-methylbenzimidazolyl) acetate (EMBA) on mild steel in hydrochloric acid. *Res Chem Intermed* 41: 4795-4823.
32. Yadav M, Sharma D, Kumar S (2015) Thiazole derivatives as efficient corrosion inhibitor for oil-well tubular steel in hydrochloric acid solution. *Korean J Chem Eng* 32: 993-1000.
33. Ramesh S, Rajeswari S (2004) Corrosion inhibition of mild steel in neutral aqueous solution by new triazole derivatives. *Electrochimica Acta* 49: 811-820.
34. Jafari H, Danaee I, Eskandari H (2014) Inhibitive Action of Novel Schiff Base Towards Corrosion of API 5L Carbon Steel in 1M Hydrochloric Acid Solutions. *Trans Indian Inst Met* 68: 729-739.
35. Chauhan LR, Gunasekaran G (2007) Corrosion inhibition of mild steel by plant extract in dilute HCl medium. *Corros Sci* 49: 1143-1161.
36. Djamel D, Tahar D, Saifi I, Salah C (2014) Adsorption and corrosion inhibition of new synthesized thiophene Schiff base on mild steel X52 in HCl and H₂SO₄ solutions. *Corros Sci* 79: 50-58.
37. Torres V, Rayol V, Magalhães M, Viana G, Aguiar L, et al. (2014) Study of thioureas derivatives synthesized from a green route as corrosion inhibitors for mild steel in HCl solution. *Corros Sci* 79: 108-118.
38. Golestani G, Shahidi M, Ghazanfari D (2014) Electrochemical evaluation of antibacterial drugs as environment-friendly inhibitors for corrosion of carbon steel in HCl solution. *Appl Sur Sci* 308: 347-362.
39. Lozano I, Mazario E, Olivares C, Likhanova N, Herrasti P (2014) Corrosion behaviour of API 5LX52 steel in HCl and H₂SO₄ media in the presence of 1,3-dibencilimidazolium acetate and 1,3-dibencilimidazolium dodecanoate ionic liquids as inhibitors. *Mat Chem Phys* 147: 191-197.
40. Olvera M, Mendoza J, Genesca J (2015) CO₂ corrosion control in steel pipelines. Influence of turbulent flow on the performance of corrosion inhibitors. *J ofoss Prev in the Process Industries* 35: 19-28.
41. Yadav M, Sharma U, Yadav PN (2013) Isatin compounds as corrosion inhibitors for N80 steel in 15% HCl. *Egyptian Journal of Petroleum* 22: 335-344.
42. Yildiz R (2015) An electrochemical and theoretical evaluation of 4,6-diamino-2-pyrimidinethiol as a corrosion inhibitor for mild steel in HCl solutions. *Corros Sci* 90: 544-553.
43. Tourabi M, Nohair K, Nyassi A, Hammouti B, Jama C, et al. (2014) Thermodynamic characterization of metal dissolution and inhibitor adsorption processes in mild steel/3,5-bis(3,4-dimethoxyphenyl)-4-amino-1,2,4-triazole/hydrochloric acid system. *J Mater Environ Sci* 5: 1133-1143.
44. Missoum N, Guendouz A, Boussalah N, Hammouti B, Chetouani A, et al. (2013) Synthesis and evaluation of bipyrazolic derivatives as inhibitors of corrosion of C38 steel in molar hydrochloric acid. *Res Chem Intermed* 39: 3441-3461.
45. Karthik G, Sundaravadevelu M, Rajkumar P (2015) Corrosion inhibition and adsorption properties of pharmaceutically active compound esomeprazole on mild steel in hydrochloric acid solution. *Res Chem Intermed* 41: 1543-1558.